
SOFA-Reconstruction Deep Markov Model (SR-DMM) for Dynamic ICU Mortality Prediction with Clinical Notes

Anonymous Author(s)

Affiliation

Address

email

Abstract

1 Timely risk updates are critical in the ICU, where rapid physiologic changes and
2 sparse, irregular documentation make multimodal early warning challenging. We
3 propose SR-DMM, a SOFA-reconstruction multimodal Deep Markov Model that
4 fuses noisy structured time series with asynchronous clinical notes in a probabilistic
5 state-space framework to update 24-hour mortality risk hourly using information
6 available up to time t. SR-DMM reconstructs SOFA-defining raw indicators (Raw6)
7 via a generative emission objective, encouraging physiologically meaningful latent
8 severity trajectories while integrating notes at the encoder/posterior to directly
9 refine state inference without heuristic decay or late fusion. In 5-fold nested
10 cross-validation, SR-DMM improves performance over common baselines.

11 1 Introduction

12 Triage and the allocation of limited medical resources across the emergency department-to-ICU
13 continuum are closely linked to patient outcomes. The ICU, in particular, requires high-frequency
14 monitoring and timely interventions, motivating risk prediction tools that can identify impending
15 deterioration early enough to guide monitoring intensity and therapeutic resources [8].

16 ICU prediction is challenging because clinical modalities differ in temporal characteristics: device-
17 derived vital signs and some laboratory measurements are relatively regular time series, whereas
18 clinical notes are free-text documents recorded irregularly. Although notes can contain condensed
19 expert assessments, integrating them with time series raises key issues in temporal alignment and
20 aggregation [3]. Moreover, real-world decision making often depends on near-term risk; accordingly,
21 early-warning benchmarks formulate the task as predicting deterioration or death within the next 24
22 hours at each time point [2].

23 Purely discriminative training on a binary outcome may overemphasize predictive cues without
24 representing the underlying evolution of physiology. Generative state-space approaches instead
25 model observations as arising from latent clinical-state dynamics. In this context, the Deep Markov
26 Model (DMM) parameterizes transition and emission distributions with neural networks and uses
27 variational inference to learn nonlinear state-space models [9].

28 The Sequential Organ Failure Assessment (SOFA) score summarizes organ dysfunction, and serial
29 SOFA changes have been associated with prognosis; Sepsis-3 operationalizes sepsis as infection with
30 organ dysfunction defined by an increase in SOFA (≥ 2) [5–7]. These foundations suggest that ICU
31 prognosis should be interpreted not only through mortality risk, but also along a clinically meaningful
32 organ-failure severity axis.

33 In this study, we propose a dynamic prediction model that integrates hourly aligned structured time
34 series (vital signs, laboratory results, and interventions) with irregular clinical notes in an MIMIC-IV
35 ICU cohort to estimate, at each time point t , the probability of death within the subsequent 24 hours.
36 The model is designed to reconstruct raw physiologic indicators underlying SOFA, encouraging latent
37 states to align with organ-dysfunction severity while supporting early-warning mortality prediction.
38 We align notes to the hourly grid and incorporate them directly into the inference encoder so that narra-
39 tive context can influence latent-state estimation, rather than injecting text via fixed heuristics such as
40 time-decay functions. By integrating multimodal evidence within a coherent state-space perspective,
41 we aim to improve the reliability and clinical meaningfulness of dynamically updated mortality risk
42 estimates in noisy, missingness-prone ICU settings. We provide an open-source implementation
43 of SR-DMM to support reproducible ICU research at (<https://anonymous.4open.science/r/sr-dmm-36BA/>).
44

45 2 Related Work

46 2.1 ICU Prediction and Research Gap

47 Dynamic ICU early-warning has been benchmarked as an hourly prediction task that estimates acute
48 deterioration or death within the next 24 hours, enabling standardized evaluation of time-varying
49 risk models [2]. Alongside risk prediction, severity scoring has been widely operationalized using
50 SOFA, a standardized index of organ dysfunction [5], with serial SOFA trajectories associated with
51 prognosis [6]. DeepSOFA further demonstrated that feeding the *SOFA-defining raw physiologic*
52 *variables* directly (rather than discrete SOFA scores) can reduce discretization-related information
53 loss and better capture temporal deterioration patterns for hourly mortality risk estimation [8]. Our
54 work shares the motivation of tracking severity over time, while extending it by (i) learning latent
55 states under an explicit **Raw6 reconstruction** objective and (ii) integrating clinical text into the same
56 state-inference process.

57 In parallel, clinical notes provide clinician interpretations and context that are difficult to infer from
58 structured signals alone, but must be mapped into fixed-dimensional representations to be used
59 by predictive models. A common fusion pipeline embeds each note and aligns/aggregates note
60 embeddings into per-timepoint vectors along the ICU timeline; for example, Khadanga et al. used
61 CNN-based note embeddings and constructed time-specific text representations via an exponentially
62 decayed weighted sum of past notes, reporting improved ICU prediction performance [3]. To address
63 irregular sampling and missingness in ICU time series more broadly, latent-variable generative
64 models—including DMM-family approaches—represent patient status as a latent trajectory and learn
65 it via amortized variational inference; Krishnan et al. introduced structured inference networks with a
66 **smoothing-style variational posterior** that leverages future observations during training to stabilize
67 latent-state estimation in nonlinear state-space models [9].

68 Despite reported gains from time series–note fusion, existing methods often implement the temporal
69 contribution of notes through heuristics. In particular, decay-based aggregation specifies a mono-
70 tonic recency assumption and introduces sensitivity to the tuned decay parameter λ [3]. Moreover,
71 when text is appended only at the prediction stage, the mechanism by which notes—as clinician
72 interpretations of patient state—modify **state inference** and representation learning remains struc-
73 turally ambiguous. This limitation is amplified by the sparsity and heterogeneity of documentation:
74 discontinuous note injection can induce artifacts, encouraging over-reliance on note-present time
75 points or leading the model to ignore text altogether. Finally, analyses that explicitly validate how text
76 alters inferred states (e.g., physiologic consistency or severity-aligned trends) remain limited. Conse-
77 quently, the underlying mechanism through which clinical text refines latent-state inference—and
78 whether improvements reflect true state refinement versus documentation-driven artifacts—remains
79 insufficiently characterized.

80 3 Data and Preprocessing

81 We constructed a multimodal ICU time-series cohort from MIMIC-IV and MIMIC-IV-Note by
82 integrating structured signals (vitals, labs, interventions) and unstructured clinical notes. We adopt
83 an hourly **dynamic prediction** setting that updates the risk of death within the next 24 hours using
84 information available up to time t . The pipeline includes cohort filtering, hourly discretization, Raw6

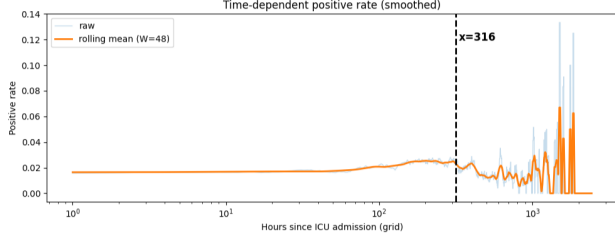


Figure 1: **Temporal changes in positive rate.** Raw time-specific positive rate (light-blue) and a 48-hour rolling mean (orange). After 316 hours (vertical dashed line), fluctuations increase due to the sharp reduction in remaining stays.

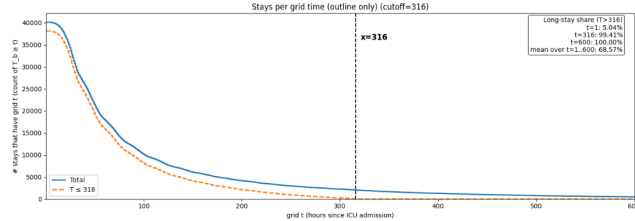


Figure 2: **Distribution of remaining ICU patients over time.** The number of patients still in the ICU decreases substantially by 316 hours (vertical dashed line), motivating the LOS cap for stability.

85 definition/alignment (SOFA components), label/mask construction, and missingness + multimodal
86 alignment [2, 8].

87 3.1 Cohort Construction, Hourly Grid, Labels, and LOS Cut-off

88 Following benchmark and prior multimodal ICU work [2, 3], we retained only each patient’s first
89 ICU stay (leakage control), excluded ICU LOS < 4 hours (early-window label instability), restricted
90 clinical text to **radiology reports in MIMIC-IV-Note**, and retained only stays with **at least one**
91 **non-UNK token** after tokenization (i.e., **non-UNK token count** ≥ 1 at the stay level). We also
92 capped LOS at 316 hours to avoid a high-variance sparsity regime. The final cohort comprised 40,098
93 stays (3,385 deaths; 8.44% stay-level). On the hourly grid, we obtained 3,712,542 time steps, of
94 which 70,331 (1.89%) were positive for “death within the next 24 hours.”

95 We discretized each ICU stay into a fixed **hourly grid** anchored at ICU admission, consistent with
96 the decompensation benchmark setup [2]. For continuous variables, we use the last measurement
97 within each hour; for event variables (procedures/medications), we encode interval-level indicators or
98 summary counts. We define $y_{b,t}$ as whether death occurs within the next 24 hours and use a validity
99 mask $\nu_{b,t}$ to exclude time points without a full 24-hour horizon from loss/evaluation. Given the low
100 base rate among valid time steps ($\approx 1.9\%$), we report PRC/AUPRC in addition to AUROC [14].

101 We cap ICU LOS at 316 hours to avoid a high-variance regime where few patients remain at risk.
102 Beyond this point, the number of ongoing stays drops sharply (Figure 2) and time-specific positive-
103 rate estimates become unstable (Figure 1), increasing sensitivity to a small long-stay subgroup and
104 degrading training stability.

105 3.2 Raw6 (SOFA Components), Clinical Text, and Missingness

106 We define **Raw6** as the six physiologic indicators underlying SOFA and use them as reconstruction-
107 aligned targets: respiration ($\text{PaO}_2/\text{FiO}_2$), coagulation (platelets), liver (bilirubin), cardiovascular
108 (MAP/vasopressors), CNS (GCS), and renal (creatinine/urine output). Raw6 was generated using
109 SOFA-related queries from the **MIT-LCP mimic-code** pipeline and mapped to the hourly grid [16].
110 This follows DeepSOFA’s motivation to avoid information loss from SOFA score discretization,
111 while differing in that Raw6 is modeled as observations to be generatively explained rather than only
112 inputs [8].

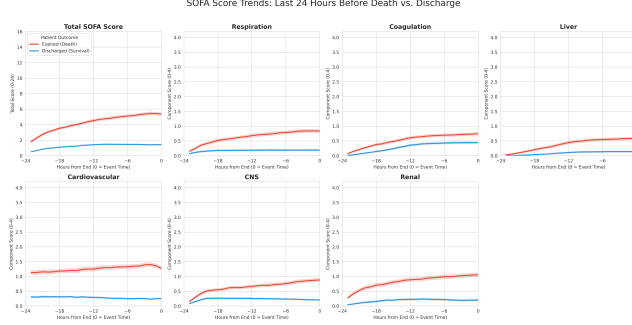


Figure 3: **Temporal trends of total and component SOFA scores in the last 24 hours.** Event-aligned mean trajectories ($t \in [-24, 0]$) show increasing severity toward death, while remaining low before discharge.

Table 1: Input composition (grouped) and observation rates.

Group	Obs. rate (%)	Examples (type)
Static demo.	90–100	age/sex/insurance (cat/cont)
Vitals (hourly)	30–95	HR, BP, RR, SpO ₂ , Temp (cont)
Labs (non-Raw6)	2–7	lactate, WBC, pH (cont)
Raw6 (SOFA comps.)	100 (binned)	P/F, PLT, bili, MAP/vaso, GCS, Cr/UO (cont/cat)
Interventions/events	0.1–40	fluids/meds/vent/proc (cat)
Note features	3–5	severity/uncertainty/abnormality (cat/cont)
Note tokens/meta	3–5	token bag + modality/region bags (emb)

113 For clinical text, we use **radiology reports from MIMIC-IV-Note** and align note timestamps to
114 elapsed hours since ICU admission, mapping them onto the hourly grid with row-level identifiers [17].
115 We define **text existence at the stay level** as having **at least one non-UNK token** after preprocessing
116 (non-UNK token count ≥ 1). Notes are structured with a local LLM (Ollama; qwen2.5-coder : 7b)
117 to produce (i) fixed-dimensional structured features and (ii) lexical tokens with negation markers
118 and UNK handling. Token sequences are serialized into EmbeddingBag-compatible arrays/offsets.
119 Exam metadata (modality/region) are normalized using the **LOINC-RSNA Radiology Playbook**
120 and encoded as separate meta-bags to preserve imaging context [19, 20]. Text inputs are aggregated
121 per hour and injected only when notes are present.

122 To handle irregular sampling, we do not forward-fill vitals/labs; instead, we provide explicit **mask**
123 **variables** so models can exploit both values and availability patterns. We additionally include a text-
124 availability indicator η_t to distinguish note-observed from note-absent intervals, following benchmark
125 and latent-variable modeling conventions where missingness itself can be informative [2, 9].

126 4 Proposed Method: SOFA Reconstruction Deep Markov Model (SR-DMM)

127 We propose the **SOFA-Reconstruction Deep Markov Model (SR-DMM)**, a probabilistic state-space
128 model for noisy/irregular ICU time series and sparse, asynchronous clinical notes. Given an hourly
129 ICU trajectory for patient b with $t = 1, \dots, T_b$, SR-DMM represents the evolving condition using
130 latent states $z_{b,t}$ and predicts the risk of death within the next 24 hours, $\hat{p}_{b,t}$. A key design is to
131 **reconstruct Raw6** (SOFA component variables) via a generative emission model, constraining the
132 latent space to preserve physiologic severity structure rather than collapsing into purely discriminative
133 shortcuts.

134 4.1 Formulation

135 Structured inputs at time t are Raw6 $x_{b,t}$ with mask $m_{b,t}$, additional continuous summaries $u_{b,t}$,
136 event features $e_{b,t}$, and static covariates s_b . Text inputs are represented by structured features $r_{b,t}$,
137 token/meta-bag embedding $g_{b,t}$, and availability indicator $\eta_{b,t}$. The time-dependent label is

$$y_{b,t} = 1 \iff \text{death occurs in } (t, t + 24\text{h}], \quad (1)$$

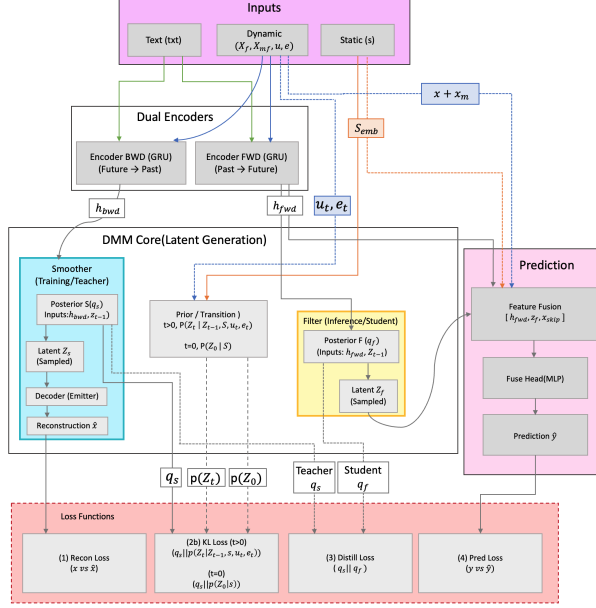


Figure 4: Overview of SR-DMM. SR-DMM reconstructs Raw6 and predicts 24-hour mortality risk on an hourly grid. Text is aligned to the grid and fused into the inference encoder to influence latent-state estimation.

138 with a validity mask $\nu_{b,t}$ to exclude time points without a full 24-hour horizon.

139 4.2 SR-DMM: Generative Model, Inference, Prediction, and Objective

140 SR-DMM defines a latent state-space model with Gaussian conditionals (diagonal covariance)
141 parameterized by neural networks. The initial latent state depends on static covariates,

$$p(z_{b,1} | s_b) = \mathcal{N}\left(\mu_{p0}(s_b), \text{diag}(\sigma_{p0}^2(s_b))\right), \quad (2)$$

142 and for $t \geq 2$ the transition depends on the previous state and covariates,

$$p(z_{b,t} | z_{b,t-1}, u_{b,t}, e_{b,t}, s_b) = \mathcal{N}\left(\mu_p(\cdot), \text{diag}(\sigma_p^2(\cdot))\right). \quad (3)$$

143 Raw6 is generated from the latent state via an emission model,

$$p(x_{b,t} | z_{b,t}) = \mathcal{N}\left(\mu_x(z_{b,t}), \text{diag}(\sigma_x^2(z_{b,t}))\right), \quad (4)$$

144 which induces an explicit reconstruction objective that aligns latent states with physiologic severity
145 structure.

146 Because exact posteriors are intractable, SR-DMM uses variational inference with a *smoothing*
147 posterior for training and a *filtering* posterior for online prediction. Both are parameterized by GRU
148 encoders operating on structured inputs and projected text. The projected text vector is

$$\sqcup_{b,t} = \phi([r_{b,t}; g_{b,t}; \eta_{b,t}]), \quad (5)$$

149 where $\phi(\cdot)$ is a lightweight projection module, enabling end-to-end learning of how notes affect
150 latent-state inference. The forward (filter) and backward (smoother; training only) encoders update

$$h_f(b, t) = \text{GRU}_{\text{fwd}}\left(h_f(b, t-1), [x_{b,t}, m_{b,t}, u_{b,t}, e_{b,t}, \sqcup_{b,t}]\right), \quad (6)$$

$$h_s(b, t) = \text{GRU}_{\text{bwd}}\left(h_s(b, t+1), [x_{b,t}, m_{b,t}, u_{b,t}, e_{b,t}, \sqcup_{b,t}]\right), \quad (7)$$

151 and define Gaussian posteriors

$$q_f(z_{b,t} | z_{b,t-1}, h_f(b, t), s_b) = \mathcal{N}\left(\mu_{qf}(\cdot), \text{diag}(\sigma_{qf}^2(\cdot))\right), \quad (8)$$

$$q_s(z_{b,t} | z_{b,t-1}, h_s(b, t), s_b) = \mathcal{N}\left(\mu_{qs}(\cdot), \text{diag}(\sigma_{qs}^2(\cdot))\right). \quad (9)$$

152 Online mortality risk prediction uses the filtering path. We form

$$\psi_{b,t} = [h_f(b, t); z_f(b, t); s_{\text{emb}}(s_b)], \quad \tilde{x}_{b,t} = g_{\text{in}}([x_{b,t}; m_{b,t}]), \quad (10)$$

153 and predict

$$\hat{p}_{b,t} = \sigma\left(f([\psi_{b,t}; \tilde{x}_{b,t}])\right), \quad (11)$$

154 where $f(\cdot)$ is an MLP and $\sigma(\cdot)$ is the sigmoid.

155 Training jointly optimizes Raw6 reconstruction, KL regularization, mortality prediction, and distilla-
156 tion from the smoother (teacher) to the filter (student):

$$\mathcal{L} = \mathcal{L}_{\text{recon}} + \beta \mathcal{L}_{\text{KL}} + \lambda_{\text{death}} \mathcal{L}_{\text{death}} + \lambda_{\text{dist}} \mathcal{L}_{\text{distill}}. \quad (12)$$

157 Reconstruction is computed only over observed Raw6 dimensions using $m_{b,t}$, mortality BCE is
158 computed only on valid time points using $\nu_{b,t}$, and distillation matches q_f to q_s while stopping
159 gradients into the teacher.

160 5 Experimental Setup and Evaluation

161 We evaluate ICU mortality forecasting as an hourly **dynamic prediction** task. At each time t , the
162 model estimates

$$\hat{p}_{b,t} = \Pr(y_{b,t} = 1 | \mathcal{I}_{b,t}), \quad (13)$$

163 where $y_{b,t} = 1$ indicates death within the next 24 hours and $\mathcal{I}_{b,t}$ denotes the information available
164 up to t [2]. We use a validity mask $\nu_{b,t}$ to exclude time points without a full 24-hour horizon and
165 compute losses/metrics only over $\{(b, t) : \nu_{b,t} = 1\}$.

166 To reduce model-selection bias, we employ **nested cross-validation**: 5-fold patient-level *outer* splits
167 for final testing and 3-fold *inner* splits for hyperparameter selection via Optuna [13]. Hyperparameters
168 are selected by maximizing inner-validation AUPRC, after which the model is refit on the full outer
169 training set and evaluated on the held-out outer test set. Results are reported as mean \pm SD across
170 outer folds. All experiments were conducted on a high-performance Linux computing environment
171 equipped with an **Intel Xeon Gold 6334 CPU (3.60GHz), 1TB RAM, and NVIDIA A30 GPUs** to
172 ensure reproducibility and computational efficiency.

173 Because positive events are rare, **AUPRC** is the primary metric, with **AUROC** reported as a comple-
174 mentary measure [14]. All metrics are computed over valid time points only.

175 We compare SR-DMM against multiple baselines and ablations under identical preprocessing, inputs,
176 masking, and evaluation. Specifically, we include (i) a heuristic-decay late-fusion baseline that
177 aggregates past note embeddings with a tuned exponential decay and fuses them with an LSTM
178 encoding of structured time series [3], (ii) a deterministic-fusion GRU baseline that concatenates
179 a per-timepoint projected text representation with the GRU hidden state for prediction, and (iii) a
180 DMM ablation without text that preserves Raw6 reconstruction, latent transition/emission structure,
181 inference encoders, prediction head, and objective. The proposed SR-DMM injects text directly into
182 the inference encoder (filter/smooth) at each time point without heuristic decay and reconstructs
183 Raw6 to constrain latent severity states; the prediction head and objective follow Section 4.

184 6 Experimental Results

185 We summarize quantitative performance, calibration, trajectory behavior, and attribu-
186 tion/representation analyses in a single unified view. Table 2 reports test performance under 5-fold
187 nested cross-validation: the proposed **Multimodal DMM** achieves the highest mean **PR-AUC** with
188 relatively low fold-to-fold variability, suggesting a stable gain under severe class imbalance.

Table 2: Quantitative comparison of dynamic mortality prediction performance on the test set under 5-fold nested cross-validation (mean \pm standard deviation).

Model	Architecture	Text Integration Strategy	PR-AUC	ROC-AUC
Baseline 1	LSTM	Heuristic Decay [3]	0.385 ± 0.013	0.913 ± 0.005
Baseline 2	GRU	Encoder Input	0.387 ± 0.020	0.914 ± 0.008
Ablation	DMM	None	0.398 ± 0.020	0.917 ± 0.007
Proposed	DMM	Encoder Input	0.410 ± 0.013	0.923 ± 0.003

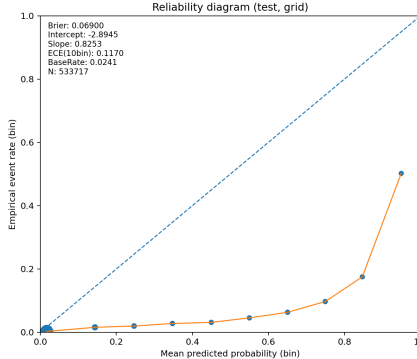


Figure 5: Reliability diagram on the test set (grid-level). In certain probability ranges, empirical event rates are lower than mean predicted probabilities, indicating mild overestimation (often associated with $\beta < 1$).

189 Beyond scalar metrics, we analyze **dynamic risk trajectories** aligned to terminal events over the last
 190 72 hours (Figure 6). The death cohort exhibits a clear upward trend toward the event, whereas the
 191 discharge cohort remains low and tends to decrease, supporting the model output as a time-varying
 192 early-warning signal.

193 We additionally evaluate **probability calibration** with a grid-level reliability diagram (Figure 5) and
 194 summarize calibration via the logistic calibration model

$$\text{logit}(y) = \alpha + \beta \cdot \text{logit}(p). \quad (14)$$

195 Calibration is computed at the **grid level**, so long-stay patients contribute more time points; thus
 196 calibration should be interpreted alongside intended threshold-based clinical use.

197 To understand model reliance on input pathways, we use IG/SHAP-style attribution (Figure 7). IG
 198 indicates that the hidden state **H** contributes most strongly, consistent with recurrent accumulation of
 199 longitudinal structured signals and note-derived context; static variables (**S**) and the skip connection
 200 (**X_FUSE**) also contribute. The *direct* contribution of the latent variable **Z** is smaller, aligning with
 201 the interpretation that z_t primarily regularizes/structures representations through Raw6 reconstruction
 202 rather than serving as a direct discriminative shortcut. Finally, we quantify how notes alter state
 203 inference via a counterfactual **representation shift** under text removal,

$$\Delta h_t = \|h_t^{\text{text}} - h_t^{\text{no-text}}\|_2, \quad (15)$$

204 and the associated prediction shift $\Delta p_t = |p_t^{\text{text}} - p_t^{\text{no-text}}|$ (Figure 8). Across alignments, shifts are
 205 larger in the death cohort, indicating stronger text-driven state updates along higher-risk trajectories.
 206 The relationship between Δh_t and Δp_t is further visualized with hexbin plots (Figure 9), showing
 207 a positive association that is stronger in the death cohort. A case study (Figure 10) illustrates that
 208 Δh_t spikes at note times and then decays, consistent with note-triggered encoder updates; text can
 209 shift risk trajectories earlier/more sharply in deterioration cases while leaving low-risk cases largely
 210 unchanged.

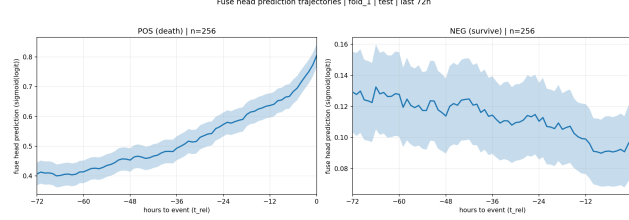


Figure 6: Dynamic mortality risk prediction trajectories in the last 72 hours prior to event. Trajectories are aligned such that the event time is $t = 0$ and visualized over $t_{\text{rel}} \in [-72, 0]$. Solid curves denote means and shaded regions indicate confidence intervals.

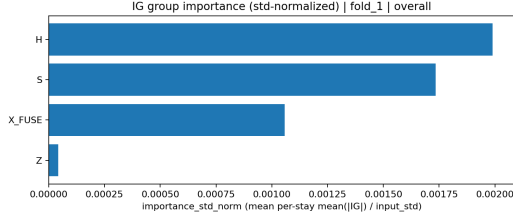


Figure 7: Overall Integrated Gradients importance by input group. IG importance is aggregated by pathway (H, S, X_FUSE, Z) using per-stay mean $|\text{IG}|$ normalized by input standard deviation. Larger values indicate higher direct output sensitivity to that pathway.

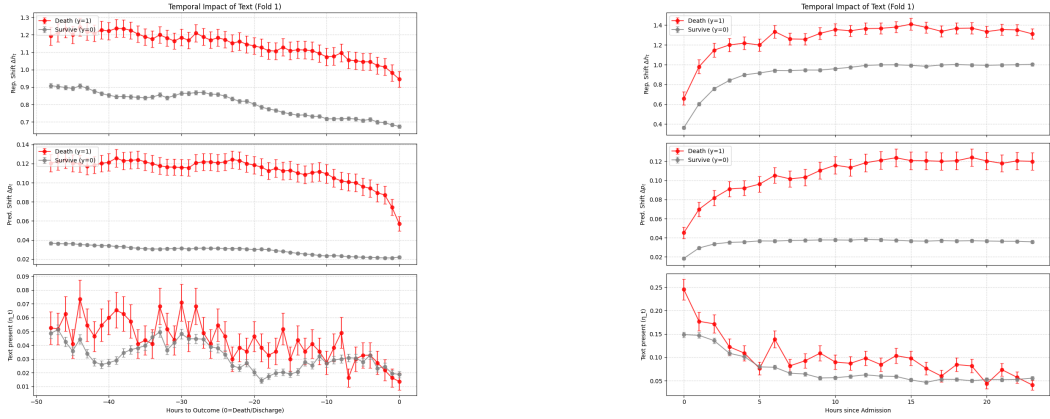


Figure 8: Temporal impact of text. (a) Outcome-aligned summaries over $[-48, 0]$ hours relative to death/discharge. (b) Admission-aligned summaries over $[0, 24]$ hours ($\text{LOS} \geq 48\text{h}$). Top: Δh_t . Middle: Δp_t . Bottom: text availability η_t . Curves are shown for death ($y = 1$) and survival ($y = 0$).

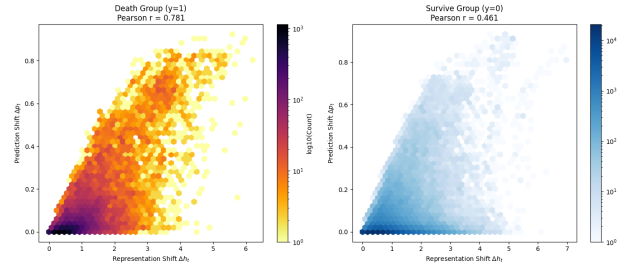


Figure 9: Relationship between representation shift and prediction shift ($\Delta h - \Delta p$ correlation). Hexbin plots show the association between Δh_t and Δp_t under counterfactual removal of text (color indicates \log_{10} frequency). Panels are stratified by outcome and Pearson correlation coefficients are reported.

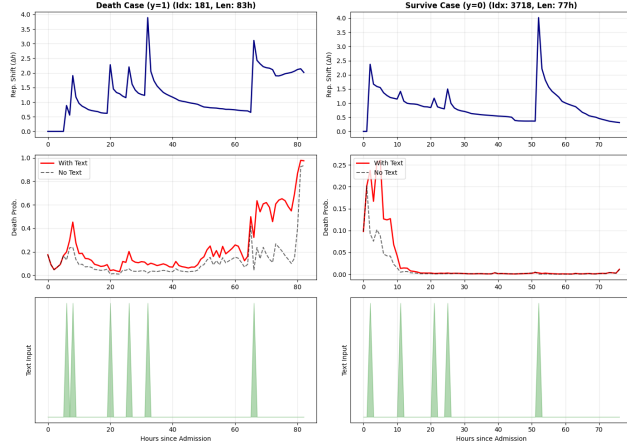


Figure 10: **Case study: text-driven latent-state updates and risk trajectory under counterfactual text removal.** Each panel shows (top) Δh_t , (middle) predicted mortality risk (with text vs no text), and (bottom) text input times for (a) a death case and (b) a discharge case.

211 7 Discussion

212 Prior multimodal ICU time-series studies often align clinical notes to structured signals using **decay-**
 213 **weighted aggregation** with a tuned decay parameter λ . While straightforward, such heuristics do
 214 not fully reflect the **irregular and sparse** occurrence of notes or the **heterogeneous documentation**
 215 **patterns** across clinicians and settings, and they typically inject text only at the prediction stage. In
 216 contrast, SR-DMM integrates text at the **encoder level**, so that notes directly influence **latent-state**
 217 **inference** within the probabilistic state-space model. This design enables end-to-end learning of how
 218 textual context calibrates the evolving patient state, avoiding fixed monotonic decay assumptions.

219 Beyond fusion, SR-DMM introduces an auxiliary objective that **reconstructs Raw6**—the physiologic
 220 variables underlying SOFA—to encourage the latent states to align with clinically meaningful **severity**
 221 **axes** and to reduce reliance on purely discriminative shortcuts. Consistent with this motivation,
 222 predicted risk trajectories exhibit clear separation between non-survivors and survivors, with non-
 223 survivors showing sharper risk escalation as endpoints approach, supporting the model output as a
 224 time-varying early-warning signal.

225 In summary, we proposed **SR-DMM**, a SOFA-reconstruction-based multimodal Deep Markov Model
 226 for hourly dynamic prediction of 24-hour mortality risk using information available up to time t . The
 227 model improves performance over comparative baselines while unifying irregular structured signals
 228 and sparse clinical notes in a coherent state-space framework. Key methodological elements include
 229 **encoder-level text fusion** (instead of late fusion with decay heuristics [3]) and a **distillation** term
 230 that transfers the advantages of smoothing-based training to filtering-time inference. Future work
 231 includes external validation beyond MIMIC-IV and leveraging posterior uncertainty (e.g., variance)
 232 for uncertainty-aware early warning and downstream clinical decision support.

233 **References**

- 234 [1] Johnson AEW, Pollard TJ, Shen L, et al. **MIMIC-IV, a freely accessible electronic health**
- 235 **record dataset.** *Scientific Data.* 2023;10:1.
- 236 [2] Harutyunyan H, Khachatrian H, Kale DC, et al. **Multitask learning and benchmarking with**
- 237 **clinical time series data.** *Scientific Data.* 2019;6:96.
- 238 [3] Khadanga S, Aggarwal K, Joty S, et al. **Using clinical notes with time series data for ICU**
- 239 **management.** In: *Proceedings of the 2019 Conference on Empirical Methods in Natural Lan-*
- 240 *guage Processing and the 9th International Joint Conference on Natural Language Processing* (EMNLP-IJCNLP). 2019. p. 6432–6437.
- 242 [4] Thorsen-Meyer H-C, Nielsen AB, Nielsen AP, et al. **Dynamic and explainable machine**
- 243 **learning prediction of mortality in intensive care: a retrospective study of time-series data**
- 244 **and ensemble learning.** *The Lancet Digital Health.* 2020;2(6):e179–e191.
- 245 [5] Vincent J-L, Moreno R, Takala J, et al. **The SOFA (Sepsis-related Organ Failure Assessment)**
- 246 **score to describe organ dysfunction/failure.** *Intensive Care Medicine.* 1996;22(7):707–710.
- 247 [6] Ferreira FL, Bota DP, Bross A, Mélot C, Vincent J-L. **Serial evaluation of the SOFA score to**
- 248 **predict outcome in critically ill patients.** *JAMA.* 2001;286(14):1754–1758.
- 249 [7] Singer M, Deutschman CS, Seymour CW, et al. **The Third International Consensus Defini-**
- 250 **tions for Sepsis and Septic Shock (Sepsis-3).** *JAMA.* 2016;315(8):801–810.
- 251 [8] Shickel B, Tighe PJ, Bihorac A, Rashidi P. **DeepSOFA: a continuous acuity score for critically**
- 252 **ill patients using clinically interpretable deep learning.** *Scientific Reports.* 2019;9:1879.
- 253 [9] Krishnan RG, Shalit U, Sontag D. **Structured inference networks for nonlinear state space**
- 254 **models.** In: *Proceedings of the Thirty-First AAAI Conference on Artificial Intelligence (AAAI-*
- 255 *17).* 2017. p. 2101–2109.
- 256 [10] Kingma DP, Welling M. **Auto-Encoding Variational Bayes.** In: *International Conference on*
- 257 *Learning Representations (ICLR).* 2014. (arXiv:1312.6114).
- 258 [11] Hinton GE, Vinyals O, Dean J. **Distilling the knowledge in a neural network.** arXiv preprint
- 259 arXiv:1503.02531. 2015.
- 260 [12] Lundberg SM, Lee S-I. **A unified approach to interpreting model predictions.** In: *Advances*
- 261 *in Neural Information Processing Systems (NeurIPS) 30.* 2017. p. 4765–4774.
- 262 [13] Akiba T, Sano S, Yanase T, Ohta T, Koyama M. **Optuna: A next-generation hyperparameter**
- 263 **optimization framework.** In: *Proceedings of the 25th ACM SIGKDD International Conference*
- 264 *on Knowledge Discovery & Data Mining (KDD).* 2019. p. 2623–2631.
- 265 [14] Davis J, Goadrich M. **The relationship between Precision-Recall and ROC curves.** In:
- 266 *Proceedings of the 23rd International Conference on Machine Learning (ICML).* 2006. p. 233–
- 267 240.
- 268 [15] Che Z, Purushotham S, Cho K, Sontag D, Liu Y. **Recurrent neural networks for multivariate**
- 269 **time series with missing values.** *Scientific Reports.* 2018;8:6085.
- 270 [16] MIT Laboratory for Computational Physiology. **mimic-code: MIMIC Code Repository**
- 271 [Internet]. GitHub repository; Accessed 2026-01-30.
- 272 [17] van Veen D, et al. **Adapted large language models can outperform medical experts in**
- 273 **clinical text summarization.** *Nature Medicine.* 2024.
- 274 [18] Yang X, et al. **GatorTron: a large clinical language model to unlock patient information**
- 275 **from unstructured electronic health records.** *npj Digital Medicine.* 2022.
- 276 [19] Vreeman DJ, Abhyankar S, Wang KC, Carr C, Collins B, Rubin DL, Langlotz CP. **The LOINC**
- 277 **RSNA radiology playbook – a unified terminology for radiology procedures.** *Journal of the*
- 278 *American Medical Informatics Association.* 2018;25(7):885–893.

279 [20] Regenstrief Institute (LOINC). **LOINC–RSNA Radiology Playbook (RSNA collaboration)**
280 [Internet]. Web resource; Accessed 2026-01-30.

281 [21] Özyurt Y, Kraus M, Hatt T, Feuerriegel S. **AttDMM: An Attentive Deep Markov Model for**
282 **Risk Scoring in Intensive Care Units.** In: *Proceedings of the ACM SIGKDD International*
283 *Conference on Knowledge Discovery and Data Mining.* 2021. p. 3452–3462.

284 **AI Co-Scientist Challenge Korea Paper Checklist**

285 **1. Claims**

286 Question: Do the main claims made in the abstract and introduction accurately reflect the
287 paper's contributions and scope?

288 Answer: [Yes]

289 Justification: The abstract and Section 1 state the proposed SR-DMM, the target task (hourly
290 24-hour mortality prediction), multimodal fusion with clinical notes, and the auxiliary Raw6
291 reconstruction objective, which match the contributions evaluated in Sections 5–6.

292 **2. Limitations**

293 Question: Does the paper discuss the limitations of the work performed by the authors?

294 Answer: [Yes]

295 Justification: Section 7 (Discussion) acknowledges limitations including single-center evalua-
296 tion on MIMIC-IV and points to future work such as external validation and uncertainty-
297 aware extensions (e.g., leveraging posterior uncertainty).

298 **3. Theory Assumptions and Proofs**

299 Question: For each theoretical result, does the paper provide the full set of assumptions and
300 a complete (and correct) proof?

301 Answer: [N/A]

302 Justification: The paper does not present formal theoretical theorems requiring proofs; it
303 provides methodological and model formulations instead.

304 **4. Experimental Result Reproducibility**

305 Question: Does the paper fully disclose all the information needed to reproduce the main ex-
306 perimental results of the paper to the extent that it affects the main claims and/or conclusions
307 of the paper (regardless of whether the code and data are provided or not)?

308 Answer: [No]

309 Justification: The paper describes the cohort definition, hourly discretization, label/mask
310 setup, and the nested cross-validation evaluation protocol (Sections 3 and 5). However, it
311 does not fully specify the complete implementation details needed to faithfully reproduce the
312 reported numbers (e.g., exact preprocessing scripts and configurations, full hyperparameter
313 search space and selected values, optimizer/training schedules, and random seeds).

314 **5. Open access to data and code**

315 Question: Does the paper provide open access to the data and code, with sufficient instruc-
316 tions to faithfully reproduce the main experimental results, as described in supplemental
317 material?

318 Answer: [Yes]

319 Justification: While the MIMIC-IV and MIMIC-IV-Note datasets are available through
320 credentialled access via PhysioNet , we provide our full codebase for data preprocessing
321 and model training at (<https://anonymous.4open.science/r/sr-dmm-36BA/>) to ensure the
322 reproducibility of our findings.

323 **6. Experimental Setting/Details**

324 Question: Does the paper specify all the training and test details (e.g., data splits, hyper-
325 parameters, how they were chosen, type of optimizer, etc.) necessary to understand the
326 results?

327 Answer: [No]

328 Justification: The paper specifies the nested cross-validation design (5-fold outer, 3-
329 fold inner), the use of Optuna for model selection, and the primary evaluation metrics
330 (AUPRC/AUROC) in Section 5. However, key training details required to fully understand
331 and replicate training are not explicitly listed (e.g., optimizer type, learning rate schedule,
332 batch size, number of epochs/early stopping, regularization settings, and the Optuna search
333 space and selected hyperparameter values).

334 **7. Experiment Statistical Significance**

335 Question: Does the paper report error bars suitably and correctly defined or other appropriate
336 information about the statistical significance of the experiments?

337 Answer: [Yes]

338 Justification: Table 2 reports mean \pm standard deviation across outer cross-validation folds,
339 which captures split-to-split variability for the main reported metrics. Figures 6 and 8 also
340 visualize trajectory summaries with shaded uncertainty bands (described as confidence
341 intervals in the captions), although the exact computation procedure is not detailed.

342 **8. Experiments Compute Resources**

343 Question: For each experiment, does the paper provide sufficient information on the com-
344 puter resources (type of compute workers, memory, time of execution) needed to reproduce
345 the experiments?

346 Answer: [No]

347 Justification: Section 5 reports the compute environment (Intel Xeon Gold 6334 CPU @
348 3.60GHz, 1TB RAM, NVIDIA A30 GPUs), but does not provide execution time per run or
349 total compute.

350 **9. Code Of Ethics**

351 Question: Does the research conducted in the paper conform, in every respect, with the
352 NeurIPS Code of Ethics <https://nips.cc/public/EthicsGuidelines>?

353 Answer: [Yes]

354 Justification: The work uses de-identified ICU EHR data accessed under standard creden-
355 tialed procedures and focuses on clinical risk prediction/interpretability. It does not involve
356 new data collection, subject recruitment, or deployment, and aims to support safer clinical
357 decision-making rather than harmful applications.

358 **10. Broader Impacts**

359 Question: Does the paper discuss both potential positive societal impacts and negative
360 societal impacts of the work performed?

361 Answer: [No]

362 Justification: The paper motivates potential positive impacts such as improved early warning
363 and resource allocation in ICUs (Sections 1 and 7). However, it does not explicitly discuss
364 potential negative societal impacts (e.g., bias/fairness concerns, misuse, over-reliance risks,
365 deployment harms) and mitigation strategies.

366 **11. Safeguards**

367 Question: Does the paper describe safeguards that have been put in place for responsible
368 release of data or models that have a high risk for misuse (e.g., pretrained language models,
369 image generators, or scraped datasets)?

370 Answer: [N/A]

371 Justification: The paper does not release a high-risk generative model or a newly scraped
372 dataset; it uses existing credentialed-access clinical data and reports an experimental study.

373 **12. Licenses for existing assets**

374 Question: Are the creators or original owners of assets (e.g., code, data, models), used in
375 the paper, properly credited and are the license and terms of use explicitly mentioned and
376 properly respected?

377 Answer: [No]

378 Justification: The manuscript credits key external assets via citations (e.g., MIMIC-IV /
379 MIMIC-IV-Note and mimic-code in the References). However, it does not explicitly list
380 the license names/versions or the full terms-of-use for each asset in the paper (beyond
381 general credentialed access expectations), so the checklist requirement of explicitly stating
382 licenses/terms is not fully met.

383 **13. New Assets**

384 Question: Are new assets introduced in the paper well documented and is the documentation
385 provided alongside the assets?

386 Answer: [Yes]

387 Justification: We release an anonymized code repository for SR-DMM (linked in the main
388 paper) that includes the implementation and supporting scripts. The repository provides
389 documentation (e.g., README) describing prerequisites, data access requirements for
390 MIMIC-IV (no redistribution), and example commands/configuration needed to run training
391 and evaluation.

392 **14. Crowdsourcing and Research with Human Subjects**

393 Question: For crowdsourcing experiments and research with human subjects, does the paper
394 include the full text of instructions given to participants and screenshots, if applicable, as
395 well as details about compensation (if any)?

396 Answer: [N/A]

397 Justification: The work is a secondary analysis of de-identified EHR data and does not
398 involve crowdsourcing or new human-subject recruitment.

399 **15. Institutional Review Board (IRB) Approvals or Equivalent for Research with Human
400 Subjects**

401 Question: Does the paper describe potential risks incurred by study participants, whether
402 such risks were disclosed to the subjects, and whether Institutional Review Board (IRB)
403 approvals (or an equivalent approval/review based on the requirements of your country or
404 institution) were obtained?

405 Answer: [N/A]

406 Justification: This is a secondary analysis of de-identified MIMIC-IV data accessed under
407 the PhysioNet data use agreement process; the study does not involve new participant
408 recruitment or intervention.